J. Plasma Fusion Res. SERIES, Vol. 5 (2002) 505–508

Effect of Poloidal Rotation on Nonlinear Resistive Wall Mode in Tokamaks

SATO Masahiko, HAMAGUCHI Satoshi and WAKATANI Masahiro
Graduate School of Energy Science, Kyoto University, Uji 611-0011, Japan

(Received: 11 December 2001 / Accepted: 19 July 2002)

Abstract

Nonlinear behavior of resistive wall modes (RWMs) has been studied in a cylindrical plasma with a poloidal rotation. Linear growth rates of RWM can be reduced by the rotation. It depends on the resistive wall position. When it is very close to the plasma column ($r_w/a \simeq 1.2$), nonlinear saturated state does not depend on the magnitude of poloidal rotation, since the poloidal rotation slows down due to the magnetic Reynolds stress. When $r_w/a \simeq 1.27$, nonlinear saturation with a small amplitude level becomes possible for a large poloidal rotation case.

Keywords:
tokamak, resistive wall mode, nonlinear MHD, poloidal plasma rotation

1. Introduction

Stability of magnetically confined plasmas is crucial for obtaining improved confinement. When a perfect conducting wall is located close to the plasma column, dangerous ideal kink modes can be stabilized. However, when the wall has a finite conductivity, resistive wall modes (RWMs) become unstable, even if the wall is close to the plasma column. The RWM grows slowly with a growth time of the order of the wall resistive decay time τ_w. For a stationary tokamak with a large bootstrap current, it is important to stabilize RWMs. Theoretical studies show that plasma rotation has stabilizing effects on linear RWM [1-3]. In DIII-D tokamak, high beta plasmas with $\beta_N > \beta_N^{\text{no wall}}$ are obtained for much longer times than τ_w when the toroidal rotation is sufficiently fast [4]. Here, β_N is a normalized beta with respect to Troyon limit and $\beta_N^{\text{no wall}}$ is the β_N limit predicted under the assumption without a wall.

When the plasma rotation decreases below a critical level, the high beta plasma phase of discharge ends due to the RWM. In order to understand these experiments, nonlinear analyses of RWMs including the plasma rotation are essential.

In Sec. **2**, the reduced MHD equations and the numerical model for studying nonlinear RWMs are described. In Sec. **3**, results of nonlinear calculations of unstable RWMs are shown. Finally, a summary is given in Sec. **4**.

2. Modeling of RWMs

The reduced MHD equations for low beta cylindrical plasmas are used [5,6]. These equations are

$$\frac{\partial \psi}{\partial t} = \frac{\partial \phi}{\partial r}\frac{1}{r}\frac{\partial \psi}{\partial \theta} - \frac{1}{r}\frac{\partial \phi}{\partial \theta}\frac{\partial \psi}{\partial r} - \frac{\partial \phi}{\partial \zeta} + \eta J - E \qquad (1)$$

$$\frac{\partial U}{\partial t} = \frac{\partial \phi}{\partial r}\frac{1}{r}\frac{\partial U}{\partial \theta} - \frac{1}{r}\frac{\partial \phi}{\partial \theta}\frac{\partial U}{\partial r} + \frac{\partial J}{\partial r}\frac{1}{r}\frac{\partial \psi}{\partial \theta} - \frac{1}{r}\frac{\partial J}{\partial \theta}\frac{\partial \psi}{\partial r} - \frac{\partial J}{\partial \zeta} + \nu \nabla_\perp^2 U + S_m, \qquad (2)$$

$$J = \nabla_\perp^2 \psi, \qquad (3)$$

$$U = \nabla_\perp^2 \phi, \qquad (4)$$

Corresponding author's e-mail: masahiko@center.iae.kyoto-u.ac.jp

©2002 by The Japan Society of Plasma Science and Nuclear Fusion Research

in a dimensionless form, where ψ is the poloidal magnetic flux and ϕ is the stream function. Here, r, θ and ζ are radial, poloidal and toroidal coordinate, respectively. In eq. (1), resistivity η is normalized to $\mu_0 a^2/\tau_{hp}$, where $\tau_{hp} = R\sqrt{\mu_0\rho}/B_0$. The length of cylindrical plasma is $2\pi R$, the plasma minor radius is a, the mass density is ρ, and the longitudinal magnetic field is B_0. In eq. (2), viscosity is denoted by ν. The source term S_m is chosen as $\nu\nabla_\perp^2 U_{eq} + S_m = 0$, where U_{eq} is a vorticity at an equilibrium state. It is noted that a poloidal rotation is introduced through U equation. In these equations, time is normalized to τ_{hp}, length to a, ψ to $B_0 a^2$, ϕ to $B_0 a^2/\tau_{hp}$ and U to B_0/τ_{hp}.

Resistivity is introduced in the vacuum region to use the pseudo-vacuum model [7,8]. Time evolution of resistivity is followed here. The equation for resistivity is assumed as

$$\frac{\partial \eta}{\partial t} = \frac{\partial \phi}{\partial r}\frac{1}{r}\frac{\partial \eta}{\partial \theta} - \frac{1}{r}\frac{\partial \phi}{\partial \theta}\frac{\partial \eta}{\partial r} + \kappa_{\parallel}\nabla_{\parallel}^2\eta + \kappa_{\perp}\nabla_{\perp}^2\eta + Q \quad , (5)$$

where the parallel diffusion coefficient of resistivity $\kappa_{\parallel}$ is normalized to R^2/τ_{hp} and the perpendicular one $\kappa_{\perp}$ to a^2/τ_{hp}. For numerical calculations $\kappa_{\parallel} = 1$ and $\kappa_{\perp} = 10^{-5}$ are assumed. The source term Q is chosen as $\kappa_{\perp}\nabla_{\perp}^2\eta_{eq} + Q = 0$, where η_{eq} is a resistivity at an equilibrium state. It is possible to include a poloidal rotation in eqs. (1), (2) and (5) with $\phi(r,t)$ since $v_\theta = -\partial\phi/\partial r$.

The pseudo-vacuum region is surrounded by the resistive wall with a finite thickness. In the resistive wall, the velocity is zero and the resistivity is independent of time. However, the poloidal flux may change in this region. It is also assumed that the outside of resistive wall is covered by a perfect conductor at $r = 2$ for simplicity. That is, the main plasma is located in the region $r \le 1$, the pseudo-vacuum in the region $1 < r < r_w$, and the resistive wall in the region $r_w \le r \le 2$, where r_w is the boundary between the pseudo-vacuum and the resistive wall.

The current profile at an equilibrium state is chosen as

$$J_{eq}(r) = \{J_{eq}(0) - J_{eq}(1)\}\{1 - r^{3.5}\}^2 + J_{eq}(1) \qquad (6)$$

for $0 \le r \le 1$, and $J_{eq}(r) = J_{eq}(1) \ll J_{eq}(0)$ for $1 < r < 2$. The resistivity profile is assumed to be proportional $1/J_{eq}(r)$ for $r < r_w$. $\eta(0)$ and the resistivity in the pseudo-vacuum region η_v are set to be $\eta(0) = 10^{-5}$ and $\eta_v = 10^{-3}$, respectively. Resistivity of the resistive wall η_w is assumed to be $\eta_w = 10^{-4}$. The profiles of q, J_{eq} and η_{eq} are shown in Fig. 1, where q is a safety factor. In Fig. 1, $q_a = 1.85$ and $r_w = 1.2$ are assumed, where q_a is safety factor at the plasma surface. The rational surface of $q = 2$ is located at $r \simeq 1.04$ in the pseudo-vacuum region.

Equations (1)-(5) are solved numerically. In our numerical code, the radial derivates is replaced with a difference approximation. The poloidal angle θ and the toroidal angle ζ are Fourier-expanded. We also assume single helicity for calculating the $(m,n) = (2,1)$ mode destabilized at the $q = 2$ surface, where m (n) is a poloidal (toroidal) mode number. The time advancement is made with a predictor-corrector method. A typical radial mesh number is 400 and 10 harmonics of the (2,1) mode are solved in nonlinear calculations.

3. Numerical Results

In this section, nonlinear RWMs are studied for the q-profile shown in Fig. 1. When a perfect conducting wall is located at $r \lesssim 1.27$ instead of a resistive wall, the ideal kink mode can be stabilized perfectly. When a

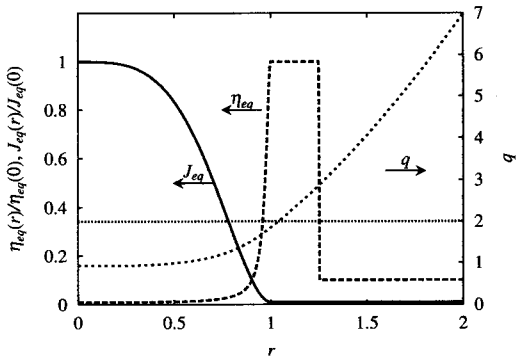

Fig. 1 Profiles of safety factor q, current J_{eq} and resistivity η_{eq} in equilibrium.

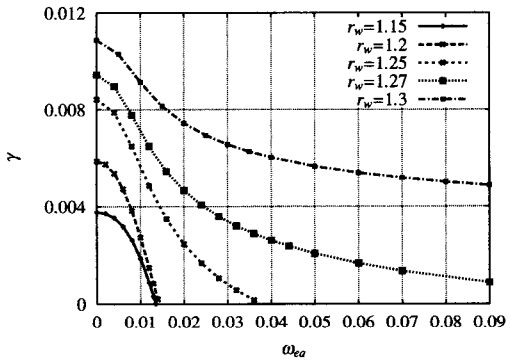

Fig. 2 Dependence of linear growth rate of RWM on the plasma rotation rate. The positions of resistive wall are 1.15, 1.2, 1.25, 1.27 and 1.3 from top to bottom.

resistive wall is assumed, RWMs become always unstable. However, RWM can be stabilized by a rigid poloidal rotation. Linear growth rates γ are plotted as a function of poloidal rotation frequency $\omega_{eq} = v_\theta / r$ in Fig. 2, where v_θ is a poloidal plasma velocity. When $\phi(r) = \phi_0 r^2$ is assumed, a rigid poloidal rotation is obtained. Here ϕ_0 is adjusted according to a value of ω_{eq}. For $r_w = 1.3$, the mode cannot be stabilized perfectly by the poloidal rotation, because the ideal kink mode with $(m,n) = (2,1)$ becomes unstable.

Figure 3 shows the time evolution of magnetic energy of $(m,n) = (2,1)$ mode for $r_w = 1.2$. For $\omega_{eq} \geq 1.2 \times 10^{-2}$ the nonlinear growth rate is enhanced when the magnetic fluctuation exceeds a critical level, and the saturated amplitude becomes comparable to that in the case of $\omega_{eq} \simeq 0$.

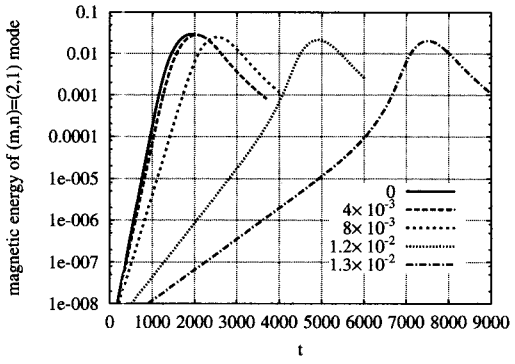

Fig. 3 Time evolution of magnetic energy of $(m,n) = (2,1)$ mode for $r_w = 1.2$ for various poloidal rotation frequencies.

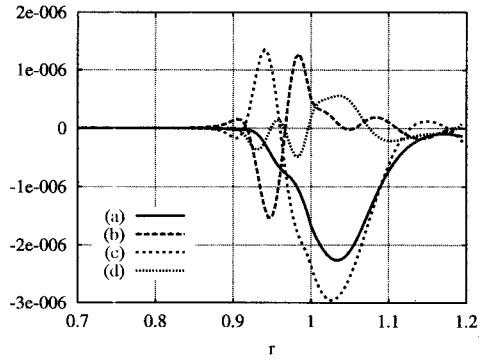

Fig. 4 Radial profiles of each term in Eq. (7) at $t = 6000$ for $\omega_{eq} = 1.3 \times 10^{-2}$. (a) $\frac{\partial \langle v_\theta \rangle}{\partial t}$, (b) $-\frac{1}{r^2}\frac{\partial}{\partial r} r^2 \langle \tilde{v}_r \tilde{v}_\theta \rangle$, (c) $-\frac{1}{r^2}\frac{\partial}{\partial r} r^2 \langle \tilde{B}_r \tilde{B}_\theta \rangle$ and (d) $-\nu \frac{d\tilde{U}_0}{dr}$.

By taking the average of eq. (2) over θ and ζ, the time evolution of average poloidal velocity $\langle v_\theta \rangle$ is described by

$$\frac{\partial \langle v_\theta \rangle}{\partial t} = -\frac{1}{r^2}\frac{\partial}{\partial r} r^2 \langle \tilde{v}_r \tilde{v}_\theta \rangle + \frac{1}{r^2}\frac{\partial}{\partial r} r^2 \langle \tilde{B}_r \tilde{B}_\theta \rangle - \nu \frac{d\tilde{U}_0}{dr}, \tag{7}$$

where $\langle f \rangle = \int_0^{2\pi}\int_0^{2\pi} f d\theta d\zeta / 4\pi^2$ and $\tilde{U}_0$ is $(m,n) = (0,0)$ component of perturbed vorticity. Figure 4 shows each terms in eq. (7) at $t = 6000$ for $\omega_{eq} = 1.3 \times 10^{-2}$. The right hand side of eq. (7) give a damping force in the vicinity of the rational surface (see Fig. 4(a)) due to the magnetic Reynolds stress (see Fig. 4(c)). The electrostatic Reynolds stress (see Fig. 4(b)) has a tendency to generate the poloidal flow. However its contribution is weak. Also the viscosity affects to generate the poloidal flow near the rational surface (see Fig. 4(d)). Figure 5 shows the time evolution of the profile of poloidal rotation velocity. The slowdown of poloidal rotation can be clearly seen as shown in Fig. 5. As the minimum of poloidal rotation velocity decreases to almost zero. Then the stabilizing effect of the poloidal rotation becomes weak. This leads to the enhanced growth rate before the saturation. It is noted that the RWM is linearly stabilized for $\omega_{eq} \gtrsim 1.4 \times 10^{-2}$ as shown in Fig. 2.

Figure 6 shows time evolution of magnetic energy of $(m,n) = (2,1)$ mode for $r_w = 1.27$. In this case, the stabilizing effect of the plasma rotation remains in the nonlinear phase for a large poloidal rotation. With the increase of ω_{eq}, the saturation level decreases significantly and the poloidal rotation survives after the nonlinear saturation.

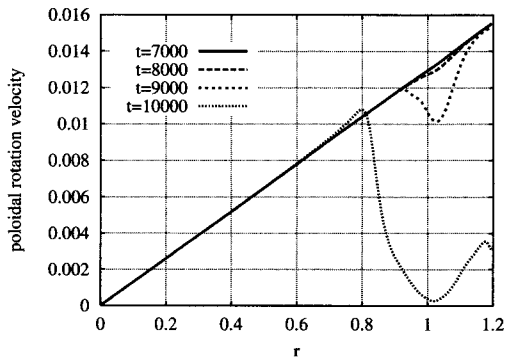

Fig. 5 Time evolution of profile of poloidal velocity for $r_w = 1.2$, $\omega_{eq} = 1.3 \times 10^{-2}$.

The maximum magnetic energy of $(m,n) = (2,1)$ mode are plotted as a function of linear growth rate in Fig. 7. For $r_w = 1.15$ and $r_w = 1.2$, saturation levels are not too small, although linear growth rates are sufficiently small. For $r_w = 1.27$, there is a large reduction of the saturation level for $\gamma < 0.004$. For $r_w = 1.27$, the dependence of the saturation level on γ changes at $\gamma \simeq 0.003$. The region with $\gamma \leq 0.003$ for $r_w = 1.27$ corresponds to the case with no large slowdown of the poloidal rotation at the rational surface in nonlinear phase. For $r_w = 1.3$, no large reduction of poloidal rotation in the nonlinear phase is seen for $\gamma < 0.006$. However, the saturation level in this region is higher than that for $\gamma < 0.003$ and $r_w = 1.27$. This is because the ideal kink mode of $(m,n) = (2,1)$ becomes unstable for $r_w > 1.27$. By comparing Fig. 7 with Fig. 2, $\omega_{eq} \gtrsim 0.04$ seems necessary to suppress saturation levels for $r_w = 1.27$ or 1.3.

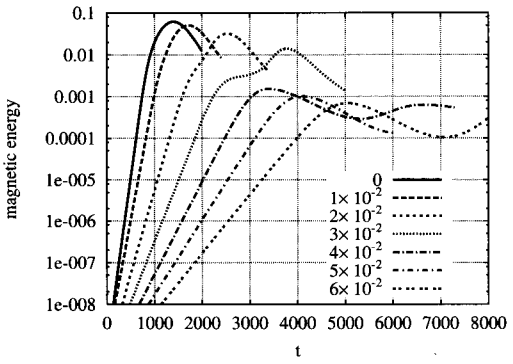

Fig. 6 Time evolution of magnetic energy of (m,n) = (2,1) mode for $r_w = 1.27$ for various poloidal rotation frequencies.

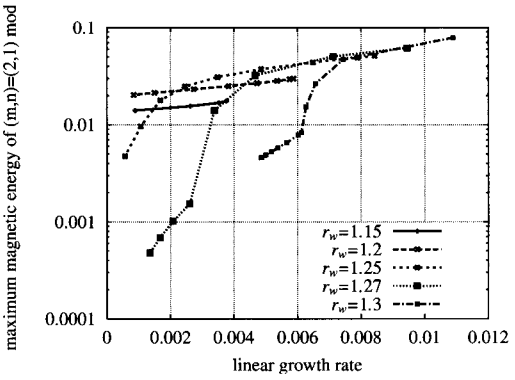

Fig. 7 Dependence of maximum magnetic energy of (m,n) = (2,1) mode on the linear growth rate.

4. Summary

When a resistive wall is placed very close to plasma surface such as $r_w \lesssim 1.2$, the reduction of poloidal rotation is significant and the RWM grows to the saturation level in the case of $v_\theta = 0$. When the distance between the plasma column and resistive wall becomes wider, the poloidal rotation velocity required to stabilize the RWM increases. However, if the poloidal rotation frequency is large, the poloidal rotation survives in the nonlinear phase. In this case, the stabilization effect of plasma rotation on the nonlinear RWM may be expected. It is remarked that the reduction of poloidal rotation comes from the magnetic Reynolds stress. Also the required poloidal velocity to affect the RWM significantly is $v_\theta/(a/\tau_{hp}) \sim 0.01$, which is nearly equal to Mach number measured with ion sound velocity for v_{pa} $(= a/\tau_{hp}) \sim C_s$ or $\beta_p \sim 1$, where β_p is a poloidal beta.

References

[1] J.M. Finn, Phys. Plasmas **2**, 198 (1995).
[2] D.J. Ward and A. Bondeson, Phys. Plasmas **2**, 1570 (1995).
[3] R. Fitzpatrick and A.Y. Aydemir, Nucl. Fusion **36**, 11 (1996).
[4] A.M. Garofalo *et al.*, Phys. Plasmas **6**, 1893 (1999).
[5] B.B. Kadomtsev and O.P. Pogutse, Sov. Phys.-JETP **38**, 283 (1974).
[6] H.R. Strauss, Phys. Fluids **19**, 134 (1976).
[7] G. Kurita *et al.*, Nucl. Fusion **26**, 449 (1986).
[8] Yu.N. Dnestrovskij *et al.*, Sov. J. Plasma Phys. **11**, 616 (1985).